Purdue University
Purdue e-Pubs

International Refrigeration and Air Conditioning Conference
School of Mechanical Engineering

2018

Impact of Surface Treatment and Geometrical Characteristics on the Condensate Retention and Frost Formation on Metal Foams

Kashif Nawaz
Oak Ridge National Laboratory, United States of America, nawazk@ornl.gov

Anthony M. Jacobi
a-jacobi@illinois.edu

Ahmed Elatar
ORNL, United States of America, elatafa@ornl.gov

Brian Fricke
Oak Ridge National Laboratory, USA, frickeba@ornl.gov

IMPACT OF SURFACE TREATMENT AND GEOMETRICAL CHARACTERISTICS ON THE CONDENSATE RETENTION AND FROST FORMATION ON METAL FOAMS

Kashif NAWAZ[1]*, Anthony JACOBI[2], Ahmed ELATAR[1], Brian FRICKE[1]
[1] Oak Ridge National Laboratory,
Oak Ridge, Tennessee, USA
(865)241-0972, nawazk@ornl.gov

[2] University of Illinois at Urbana Champaign,
Urbana, Illinois, USA
(217)333-4108, a-jacobi@ornl.gov

[1] Oak Ridge National Laboratory,
Oak Ridge, Tennessee, USA
(865)241-0972, elatafa@ornl.gov

[1] Oak Ridge National Laboratory,
Oak Ridge, Tennessee, USA
(865)576-0822, frickeba@ornl.gov

* Corresponding Author

ABSTRACT

Metal foams has been considered as promising materials for multiple thermal applications including air-cooling. Their use in such an application requires a detailed analysis of the condensate retention and frost accumulation in the metal foam pores. The current study is focused on the impact of surface treatment on the performance of metal foams when they are deployed in dehumidifying and frosting environment. Aluminum and cooper foam samples have been treated to achieve hydrophilic, hydrophobic and super hydrophobic characteristics and associated condensate retention and frost accumulation on the surface has been measured at various relative humidity and base temperature conditions. High resolution imaging techniques has been used to illustrate the impact of surface treatment. Along with the surface treatment, the impact of metal foam geometry (porosity and pore size) has been highlighted as well and the findings have been summarized in form of guidelines for the application of metal foam in air cooling application where the condensation and frost formation cannot be avoided.

1. INTRODUCTION

Metal foams have been considered for numerous thermal applications including cryogenics, combustion chambers, catalytic beds, compact heat exchangers for airborne equipment, air cooled condensers and compact heat sinks for power electronics. Although the development is in-progress to resolve some manufacturing and implementation issues, these materials have shown remarkable performance for heat exchangers and heat sinks [1]. Characteristics such as open porosity (Fig. 1), low relative density, high thermal conductivity of the cell edges, large accessible surface area per unit volume (Fig. 2) [2-7], and the ability to mix the cooling fluid are important for development of efficient, compact, and light-weight thermal management devices. Several studies have concluded that metal foams have relatively large pressure drop per unit length which is caused by complex geometry of the foams. However, the complex tetrakaidecahedron structure also results in high degree of boundary layer restarting and wake destruction by mixing [8-17]. Overall the increase in pressure drop is mitigated by the considerably higher heat transfer coefficients.

Dai *et al.* [16] compared the heat transfer and pressure drop performance of metal-foam heat exchangers to another state-of-the-art heat exchanger. In the analysis, two heat exchangers were subjected to identical performance requirements, and the resulting volumes, masses, and costs were compared. Metal foam heat exchangers were found to meet the thermal requirements at lower volume and mass, but at a higher cost. Nawaz *et al.* [17] considered open-cell aluminum metal foam as a highly compact replacement for conventional fins in heat exchangers. Heat transfer and pressure drop data for different PPI metal foam heat exchanger were evaluated by wind-tunnel experiments in order to make the comparison with the louver-fin heat exchangers.

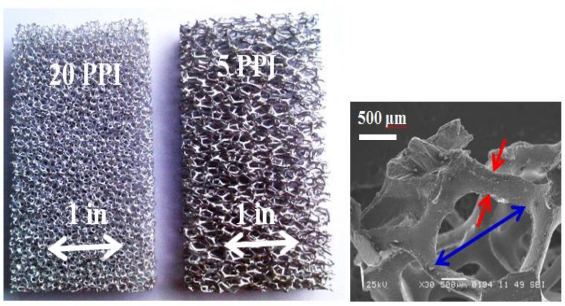

(a) (b)

Fig. 1: Definition of length scale for metal foams (a) 20 and 5 PPI (b) Pore diameter (blue), strut diameter (red)

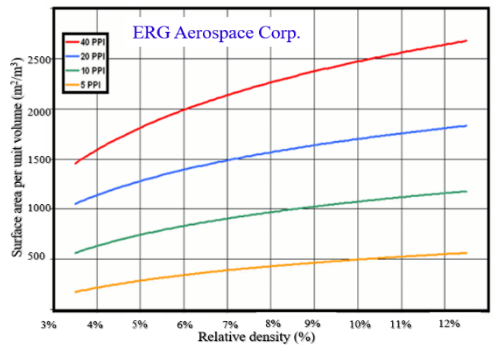

Fig. 2: Surface area per unit volume for different types of metal foams.

Some studies have been conducted to investigate the performance of metal foam heat exchangers under dehumidifying conditions [18,19]. When the heat exchangers operating under dehumidifying conditions [20,21] the condensate accumulates on the fin surface and ultimately leads to additional pressure drop. Furthermore, it also adds to additional resistance to heat transfer, which can have a profound impact on the overall performance of heat exchangers [22]. Some of the recent studies have shown that the water retention in metal foam increases as the porosity decreases [22,23] and the water drainage characteristics of the metal foam heat exchanger are better than that of the fin-tube heat exchanger [23].

Although there are multiple studies on the evaluation of the performance of metal foams heat sinks and heat exchangers under dry operating conditions., there is rare information available about the performance when these devices operate in dehumidifying and frosting conditions. For the large-scale deployment of these novel materials, it important to determine their performance since condensate formation, retention and drainage are critical factor which are absent as they operate under dehumidifying conditions. Similarly, frost growth is unavoidable when the operating temperature are very low. In the current study, the condensate retention and frost formation of metal foam has been evaluated through an experimental process and associated impact are explained in detail.

2. CONDENSATE DRAINAGE PERFORMANCE

2.1 Experimental Apparatus

Condensate retention and drainage behavior is a critical parameter impact the performance of heat exchanger during condensing conditions. Condensate retention and the drainage rate were assessed through the dynamic dip test (Fig. 3). The setup consisted of a large water reservoir, a smaller submerged air tank to control the water level using pressurized air, and a supporting structure for mounting and weighing the test sample. The volume of the large reservoir was about 1 m^3 and the smaller displacement tank was 0.4

m^3. A pipe of 50 mm diameter was used as an air passage. The test sample was suspended from an electronic balance using a fixed acrylic frame and simple mounting hardware. A dry test metal foam was suspended over the water reservoir and the alignment was confirmed. After the balance was zeroed, the water reservoir was raised to immerse the specimen. The water was agitated to remove air trapped in the metal foam sample, before the reservoir was lowered. Beginning at the instant when the water level reached the bottom of the heat exchanger, mass readings were recorded at 5-s intervals for 90 s and then at 30-s intervals for additional 240s. A computer-based data acquisition system was used for monitoring and recording data. The balance was calibrated to an accuracy of ±0.1 gram.

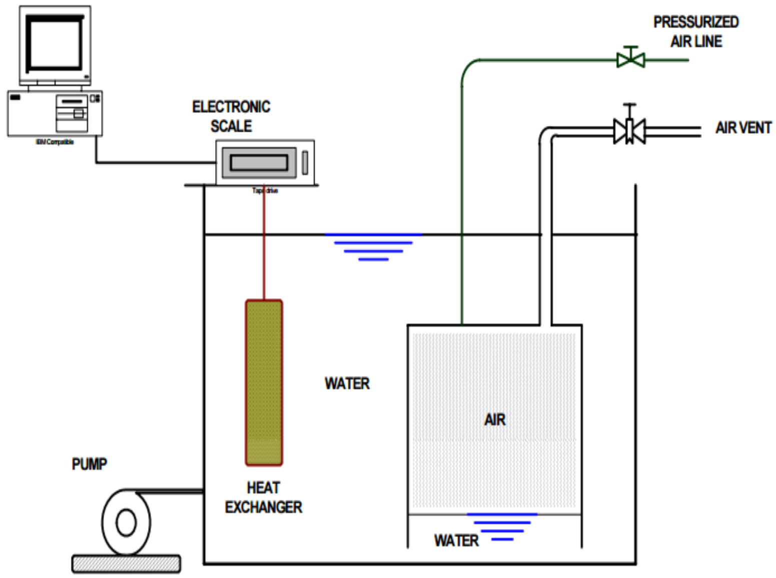

Fig. 3: Dynamic dip apparatus to analyze the condensate retention

2.2 Samples Characteristics

Five different test samples have been used in the experiments for the dynamic dip testing, which were 75 mm long, 25.4 mm wide and 13 mm thick. Estimated geometric data for the specimens are provided in Table 1, where the average strut diameter, d_f, pore diameter, d_P, and porosity are provided. The foam samples where fixed between flat faux tubes, with the longest dimension aligned with gravity for the dynamic dip tests.

Table 1: Characteristics of metal foam samples

Sample #	Porosity	PPI	d_f *(mm)*	d_P *(mm)*
1	0.953	5	0.50	4.02
2	0.942	10	0.40	3.13
3	0.933	20	0.30	2.70
4	0.927	40	0.25	2.02
5	0.913	45	0.20	2.00

2.3 Impact of Pore Size on Condensate Drainage

Porosity is an important factor in characterizing the metal foams, though there are other criteria available for distinguishing different types. Generally metal foams are produced in 5, 10, 20 and 40 PPI sizes (where PPI is the pores per inch). This characterization is an approximation made by counting the pores in one inch along one dimension, so foam characterized by 5PPI will have 5 pores in a length of 1 inch.

The water retention in grams per unit volume for samples with five different porosities is presented in Fig. 4. Experiments on all the samples were conducted under same conditions and equal time was given to analyze the steady state behavior for the water retained in the sample. It can be observed from the data that porosity has a noticeable impact on the water retention, as for a 45 PPI sample with smaller sized pores, water retention is large as compared to the 10 PPI sample, which shows the least retention. Fig. 5 shows the test samples and an obvious difference in geometry can be observed.

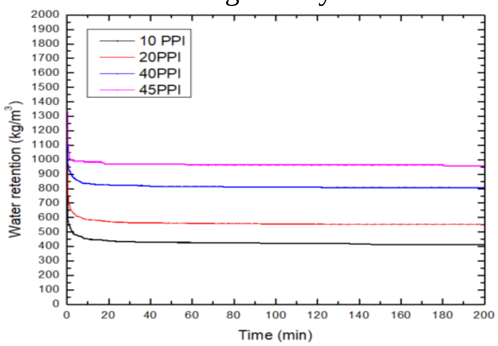

Fig. 4: Water retention for metal samples with different porosities

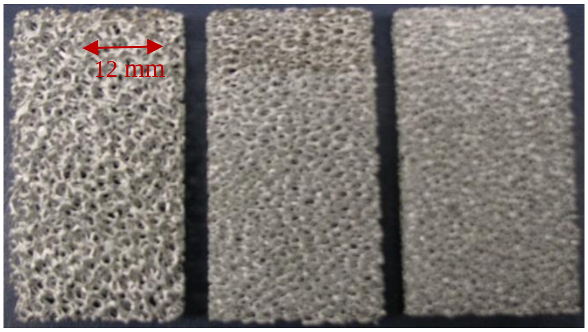

Fig. 5: Metal foam samples with different porosities (10, 20 and 40PPI)

2.4 Impact of Surface Treatment on Condensate Drainage

Surface treatments are sometimes conducted to improve the water drainage performance of compact heat exchangers. In order to explore the impact of surface treatment on condensate drainage a beomite treatment was implemented. In this approach the samples were washed in boiling soapy water for about 5 minutes. After this treatment the sample surface was considerably altered, as can be seen in Fig. 6. In order to quantify the effect of this treatment on water drainage, the dynamic dip test was carried out on treated samples and compared to an untreated samples with comparable geometry (pore size and porosity). The results for the 10 PPI sample before and after treatment are compared in Fig. 7. Surprisingly, the Beomite process, which typically promotes drainage, had an adverse effect on the drainage behavior; the treated sample held more water compared to an untreated sample. It can be concluded that such surface treatment increased the hydrophobicity of the metal foam.

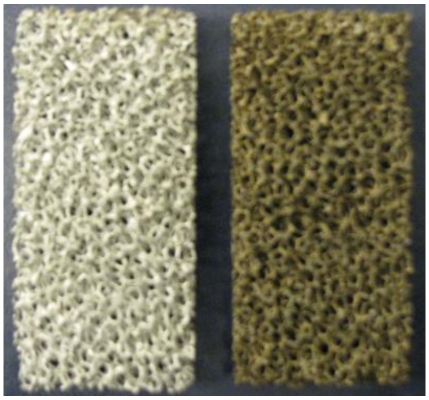

Fig. 6: 10 PPI Metal foam sample before and after treatment

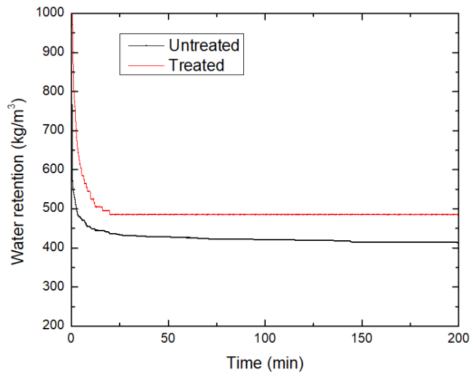

Fig. 7: Water retention for treated and untreated samples

2.5 Impact of Combing Samples with Different Pore Sizes

Its important to fully understand the potential wicking effect as it can considerably alter the condensate drainage behavior. To accomplish this metal foams with different porosities were placed together to achieve a sample with variable pore size and dynamic dip tests were conducted using five layers of foam with different porosities. For baseline testing five layers of metal foams with 5 PPI, 10 PPI, 20 PPI, 40 PPI and 45 PPI were tested. The sample with variable pore size had the same geometry as baseline samples (length, width and thickness), however instead of uniform pore size sizes it had a variable pore size (10-20-40-20-10 PPI) such that the smaller pore size block (40 PPI) was placed in the center. The results for the dynamic dip test experiments are shown in Fig. 8. As expected, the 40 PPI sample held more water than the 10 PPI sample, However, the sample consisting of variable pore size block showed a remarkable drainage performance. The amount of water retained was nearly the same as that of the 10 PPI sample after achieving the steady state. This effect suggests that combinations of foam could be used in designs where heat transfer, pressure drop, and condensate retention effects are all important.

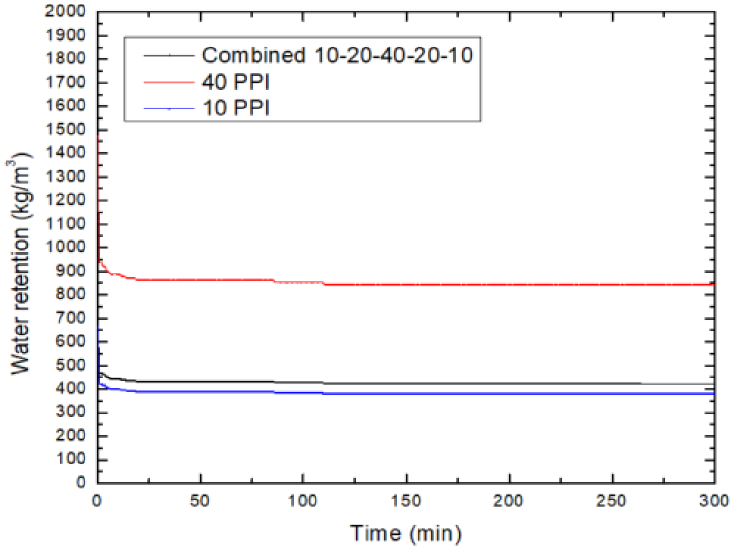

Fig. 8: Water retention for combined samples

3. FROST FORMATION ON METAL FOAMS

3.1 Experimental Apparatus

The frost growth experiments were conducted in a closed psychrometric chamber where the conditions such as dry bulb temperature and relative humidity were controlled to have a comparable environment for all the experiments. The test samples were attached to a cold plate using a high thermal conductivity paste. The cold plate temperature is controlled by circulating cold fluid provided a water bath. The change in the mass due to the frost growth was monitored and recorded using a high precision balance (Fig. 9). The test samples were aluminum and copper foams with different PPI i.e., pore sizes (75 mm long, 25.4 mm wide and 13 mm thick). All the samples were cleaned using isopropanol. A high-resolution camera was used to capture the images at various time period to observe the frost growth on metal foam surface.

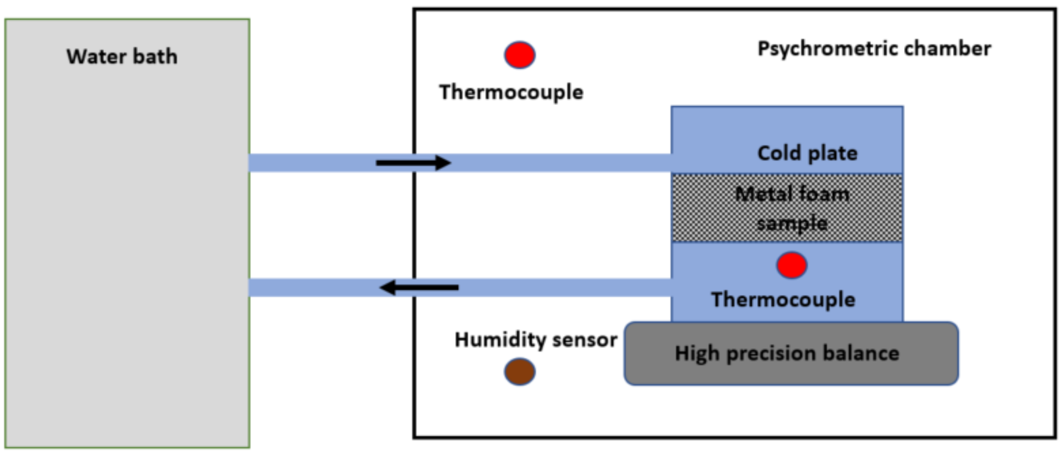

Fig. 9: Water retention for combined samples

All the experiments were conducted under natural convection process i.e., no air flow was induced as the frost grew on the metal foam surface. The relative humidity and temperature in the psychrometric chamber was controlled at 40% and 32 C. The plate temperature was maintained at -10 C using the glycol solution coming from the water bath. A computer-based data acquisition system was used for monitoring and recording data. The balance was calibrated to an accuracy of ±0.01 gram.

3.2 Frost Formation on Aluminum Metal Foams

Aluminum metal foam with three different pore sizes were used in the first set of experiments including 5,10 and 20 PPI. Figs. 10 to 12 present the images of the test samples at various time of operation. It can be observed from the figures that frost start growing the intersection of adjacent ligaments for the all the test samples. Additionally, the frost growth rate is relatively faster on metal foams with relatively smaller pore size (higher PPI). Another critical observation is frost density. As it appears from the images the frost density was almost similar for all the foam samples. Fig. 16 present the mass of frost grown on various test samples at different time intervals. A test sample with 5PPI metal has the least amount of frost compared to other two samples. This can be attributed to the relatively lower number for intersection point for a 5PPI metal foam among metal foam ligaments. As indicated above for the aluminum samples the frost started growing at the intersection points, so a higher density of such intersection means relatively larger number of frost "nucleation sites".

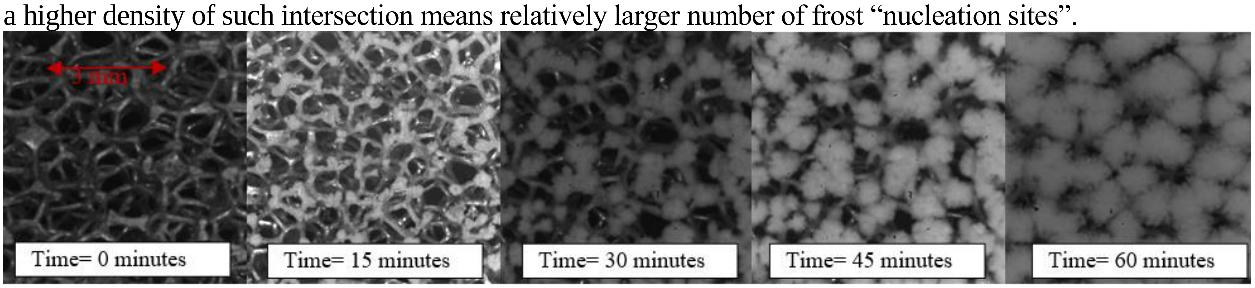

Fig. 10: Frost growth on a 5 PPI aluminum foam

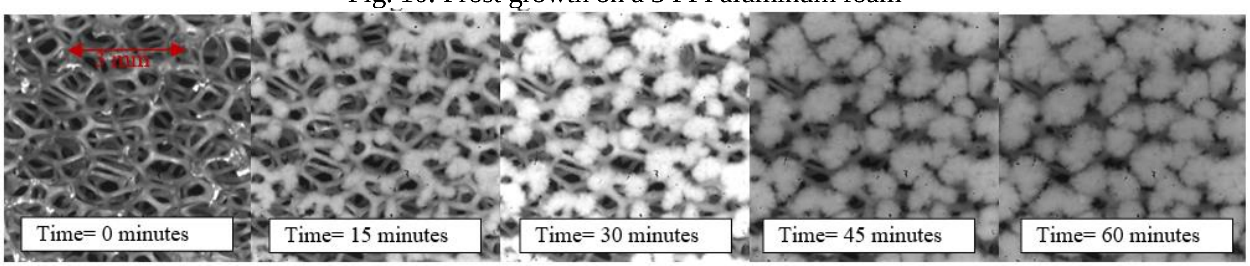

Fig. 11: Frost growth on a 10 PPI aluminum foam

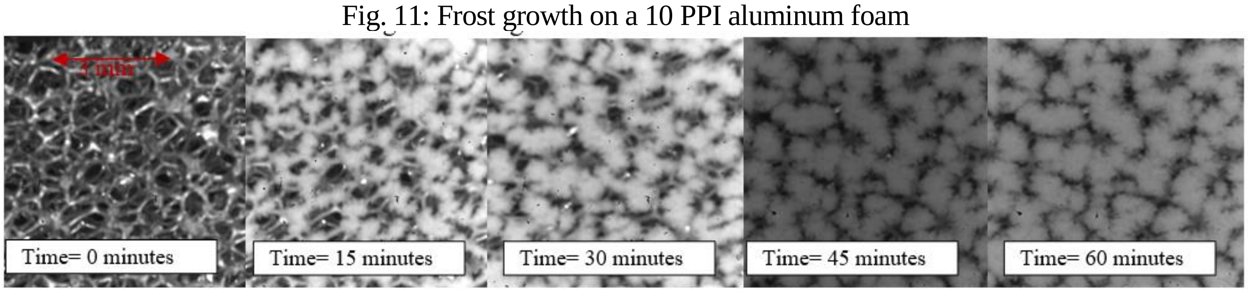

Fig. 12: Frost growth on a 20 PPI aluminum foam

3.3 Frost Formation on Copper Metal Foams

Another set of copper metal foams were used for frost experiments. The test conditions were comparable for all the experiments. Figs. 13 to 16 present the images of copper foam at various stage of frost growth process. Some interesting observations can be made from the analysis of these images. First, unlike aluminum foam, the frost growth was more uniform throughout the cell structure i.e., even though the frost growth started at the ligament intersection, however, the frost started growing in the ligaments as well. Additionally, although the frost density for all copper samples appears comparable, the frost on the copper surface appeared more fluffy as it appears from the needle like crystals on the copper foam samples. Fig. 17 compares the amount of frost grown at different samples recorded at various stages of the experiments. It is obvious from the measurements that unlike for aluminum foam, PPI or the pore size was not very critical since all the samples accumulated almost comparable frost mass. This can be associated with relative better thermal conductivity of copper foam compared to aluminum foam. Based on such observation it can be summarized that as the thermal conductivity of the metal foam increases, the geometrical parameters such as ligament size and pore size become less critical. Its worth noting that all these experiments were conducted under natural convection which means there was no air flow involved. While the pore size showed it impact on frost growth rate on the aluminum foam, the frost growth process becomes a strong function of pore size when it's a forced convection. It has been noted by the authors that the physics of frost growth during forced convection is completely different from the that during the natural convection.

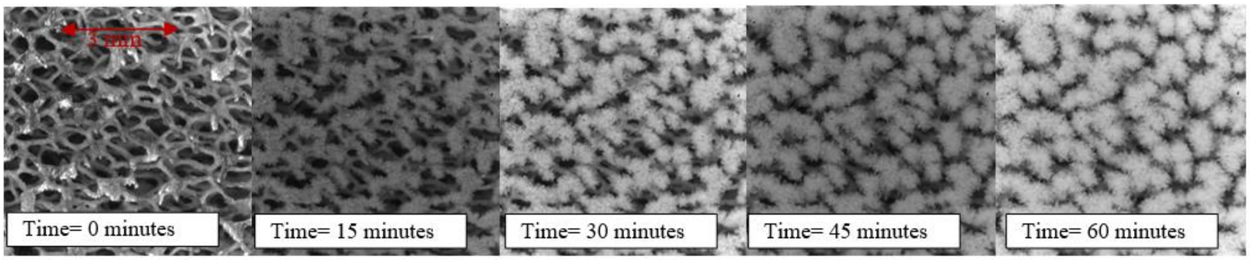

Fig. 13: Frost growth on a 10 PPI copper foam

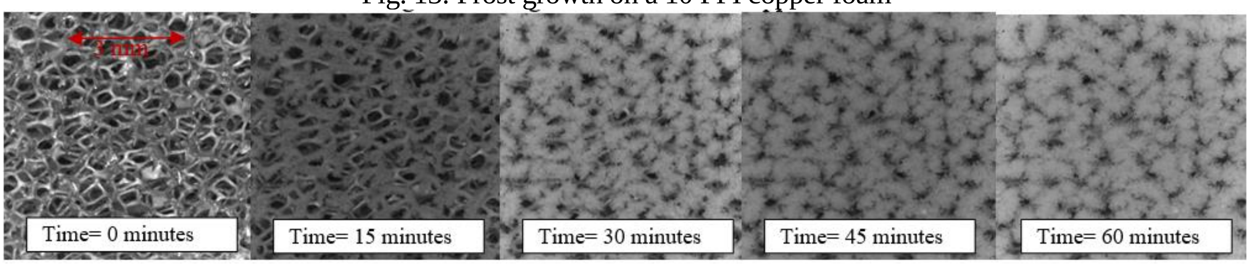

Fig. 14: Frost growth on a 20 PPI copper foam

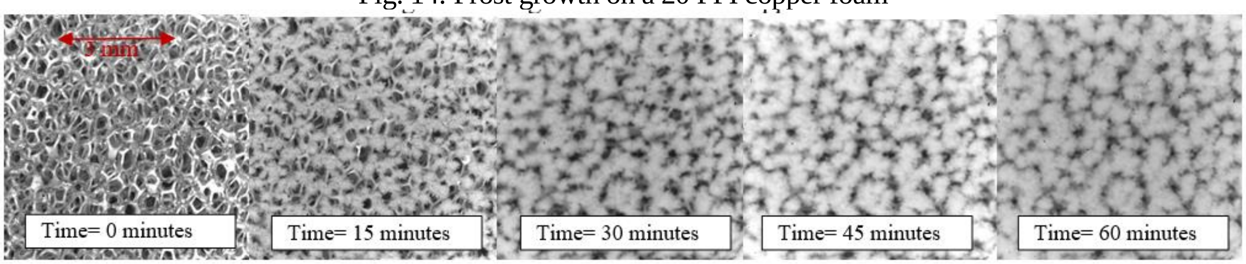

Fig. 15: Frost growth on a 40 PPI copper foam

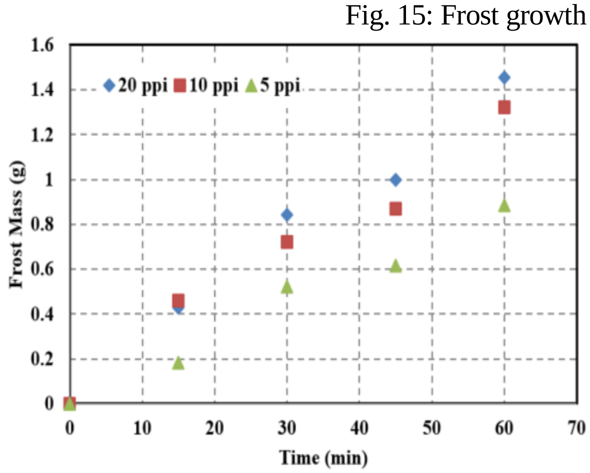

Fig. 16: Frost mass on aluminum foam samples

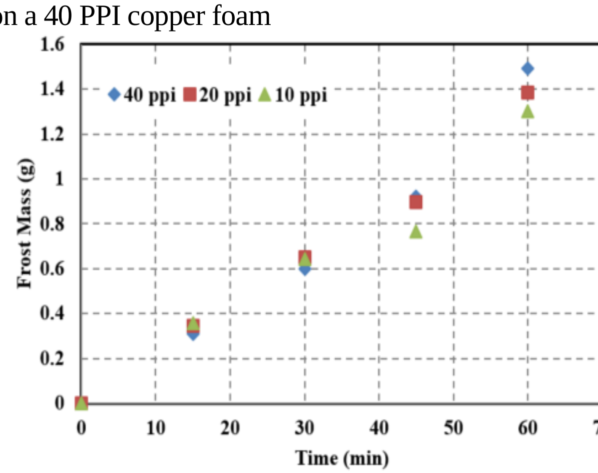

Fig. 17: Frost mass on copper foam samples

4. CONCLUSIONS

An experimental study has been conducted to analyze the impact of metal foam geometry when they are used in condensing and frosting conditions. Condensate drainage highly depends on the pore size of the metal foam and drainage performance of 5 PPI is considerably better compared to 40 PPI metal foam. The surface treatment and variable pore size can also lead to noticeable changes in condensate drainability. The frost growth starts at the intersection of metal foam ligaments and the phenomena is more obvious for aluminum foam compared to the copper foam. The frost is more structured (crystals are obvious) for growth on the copper foam compared to the aluminum foams.

NOMENCLATURE

d_f	Ligament diameter	(m)
d_P	Pore diameter	(m)

REFERENCES

[1] Han, X., Wang, Q., Park, Y., T' Joen, C., Sommers, A., Jacobi, A. M., A review of metal foam and metal matrix composites for heat exchangers and heat sinks (Review), *Heat Transfer Engineering*, 33, pp. 991-1009 (2012).

[2] Perrot, C., Panneton, R., Olny, X., Periodic unit cell reconstruction of porous media: Application to open-cell aluminum foams, *Journal of Applied Physics*, 101, pp. 13538 (2007).

[3] Bock, J., Jacobi, A. M., Geometric classification of open-cell metal foams using X-ray micro-computed tomography, *Materials Characterization*, 75, pp. 35-43 (2013).

[4] Nawaz, K., Schmidt, S., Jacobi, A. M., A Parametric Study about Mass Diffusion Coefficient of Desiccants for Dehumidification Applications: Silica Aerogels and Silica Aerogel Coatings on Metal Foams, *HVAC and R Research, Special issue: Advances in refrigeration and heat transfer engineering*, 21, pp. 637-647 (2015).

[5] Nawaz, K., Schmidt, S., Jacobi, A. M., Effect of catalyst and substrate on the moisture diffusivity of silica-aerogel-coated metal foams", *International Journal of Heat and Mass Transfer*, 73, pp. 634-644 (2014).

[6] Nawaz, K., Bock, J., Jacobi, A. M., Experimental studies to evaluate the use of metal foams in highly compact air-cooling heat exchangers, *Proceedings of 13th International Refrigeration and Air Conditioning Conference* (2012).

[7] Zhao, C. Y., Review on thermal transport in high porosity cellular metal foams with open cells, *International Journal of Heat and Mass Transfer*, 55, pp. 3618-3632 (2012).

[8] Nawaz, K., *Aerogel coated metal foams for dehumidification applications*, Ph.D. Thesis, University of Illinois at Urbana-Champaign, USA (2013).

[9] Ejlali, A., Hooman, K., Gurgenci, H., Application of high porosity metal foams as air-cooled heat exchangers to high heat load removal systems, *International Communications in Heat and Mass Transfer*, 36, pp. 674-679 (2009).

[10] Boomsma, K., Poulikakos, D., Zwick, F., Metal foams as compact high performance heat exchangers, *Mech. Mater.*, 35 (12), pp. 1161-1176 (2003).

[11] Ribeiro, G. B., Barbosa, J. R., Prata, A. T., Performance of microchannel condenser with metal foams on the air-side: Application in small scale refrigeration systems, *Applied Thermal Engineering*, 36, pp. 152-160 (2012).

[12] Calmidi, V. V., Mahajan, R. L., Forced convection in high porosity metal foams, *ASME Journal of Heat Transfer*, 122, pp. 557–565 (2000).

[13] Dukhan, N., Chen, K. C., Heat transfer measurements in metal foam subjected to constant heat flux, Experimental Thermal and Fluid Science, 32, pp. 624–631 (2007).

[14] Boomsma, K., Poulikakos, D., On the effective thermal conductivity of a three dimensionally structured fluid-saturated metal foam, *International Journal of Heat and Mass Transfer*, 44, pp. 827–836 (2001).

[15] Han, X., Nawaz, K., Jacobi, A. M., Open-cell metal foam for use in dehumidifying heat exchanger, *Proceedings of 13th International Refrigeration and Air Conditioning Conference* (2012).

[16] Dai, Z., Nawaz, K., Park, Y., Chen, Q., Jacobi, A. M., A comparison of metal-foam heat exchangers to compact multilouver designs for air-side heat transfer applications, Heat Transfer Engineering, 33 (1), pp. 21-30 (2012).

[17] Nawaz, K., Bock, J., Jacobi, A. M., Thermal-hydraulic performance of metal foam heat exchangers under dry operating conditions, *Applied Thermal Engineering*, 119 (5), pp. 222-232 (2017).

[18] Hu, H, Weng, X., Zhuang, D., Ding, G., Lai, Z., Xu, X., Heat transfer and pressure drop characteristics of wet air flow in metal foam under dehumidifying conditions, Appl. Therm. Eng. 93 (2016) 1124-1134.

[19] Costa, C. A. S., Miranda, V., Mantelli, M. B. H., Da Silva, A. K., Modenesi, C. R., Furlan, L. T., Experimental study of flexible, unstructured metal foams as condensation structures, Exp. Ther Fluid Sci. 57 (2014) 102-110.

[20] Zhang, L., Dang, C. Hihara, E., Performance analysis of a no-frost hybrid air conditioning system with integrated liquid desiccant dehumidification, Int. J. Refrig. 33 (1) (2010) 116–124.

[21] Zhuang, D., Ding, G., Hu, H., Fujino, H., Inoue, S., Condensing droplet behaviors on fin surface under dehumidifying condition: Part I: Numerical model, Appl. Therm. Eng. 2015.

[22] Kaviany, M., Principles of Heat Transfer in Porous Media, Springer-Verlag, New York, 1995, Chapter. 2.

[23] Han, X., Nawaz, K., Open-cell metal foam for use in dehumidifying heat exchanger, International Refrigeration and Air Conditioning Conference, Purdue, USA, Paper 1312, 2012.

ACKNOWLEDGMENT

Authors acknowledge support provided by the Air Conditioning and Refrigeration Center (ACRC, an NSF-founded Industry-University Cooperative Research Center) and by the DOE Building Technologies Office and the Technology Manager, Antonio Bouza.